Existence of the Na−$H^{\delta-}$···$H^{\delta'+}$−O Dihydrogen Bond in the Hydrogenation Process by Na_2O: A First-Principles Identification

Xin-Bo Zhang,[†] Si-Qi Shi,[†] Ling Jiang,[†] Song Han,[†] Yukinari Kotani,[‡] Tetsu Kiyobayashi,[†] Nobuhiro Kuriyama,[†] Tetsuhiko Kobayashi,[†] and Qiang Xu*[,†]

National Institute of Advanced Industrial Science and Technology (AIST), 1-8-31 Midorigaoka, Ikeda, Osaka 563-8577, Japan, and Toyota Motor Corporation, Susono, Shizuoka 410-1193, Japan

Received: September 12, 2006; In Final Form: February 2, 2007

The adsorption and dissociation of H_2 on the Na_2O (110) surface have been studied with the first-principles molecular dynamics method. It is found that the adsorption configuration is energetically preferred when the H_2 molecule is situated at the bridge site of the Na and O atoms, which indicates the formation of a Na−$H^{\delta-}$···$H^{\delta'+}$−O dihydrogen bond, as confirmed by the charge distribution features and bond lengths between the concerned atoms. The molecular dynamics simulations reveal the dissociation of the newly discovered H···H dihydrogen bond, which facilitates the $Na_2O + H_2 \rightarrow NaH + NaOH$ reaction.

1. Introduction

Finding effective hydrogen storage materials is one of the most difficult challenges facing the hydrogen-powered society, and its solution requires breakthroughs in material performance coming from wide-range innovative basic research that looks beyond the currently known storage materials.[1,2] Subsequently, a novel dihydrogen bond that seems to be general for interactions between hydrides with hydridic hydrogen and classical hydrogen bond donor groups has been reported.[3−7] Just as classical H bonds play an important role in the field of hydrogen storage, the discovery of the dihydrogen bonds may potentially lead to ways of synthesizing and promoting the chemical reactivity of novel hydrogen storage materials.

We have recently found that sodium oxide can reversibly take up 3.0 wt % hydrogen to form sodium hydride and sodium hydroxide, thus extending the hydrogen storage materials, which have been limited thus far in elements before group 15, to the group 16 elements.[8] In addition, on the basis of our results, we proposed that a reaction mechanism, with a Na−$H^{\delta-}$···$H^{\delta'+}$−O reaction intermediate, involving dihydrogen bonding between the negatively charged hydrogen atom bonded to sodium and the positively charged hydrogen atom bonded to oxygen, might play an important role in both the hydrogenation and the dehydrogenation processes of the Na−O−H system. However, to the best of our knowledge, the existence and chemical reactivity of dihydrogen bond on metal oxide surfaces have not been reported.

During the past few years, theoretical calculations based on the density functional theory (DFT) have made an important impact on the understanding of structure, stability,[9,10] and chemical reactivity[11] of hydrogen materials. In the present paper, we focus on the adsorption and dissociation of H_2 on the Na_2O (110) surface, to elucidate the existence of the Na−$H^{\delta-}$···$H^{\delta'+}$−O dihydrogen bond when H_2 is adsorbed on the Na_2O (110) surface and the role of the dihydrogen bond in the hydrogenation of Na_2O. The reason we choose (110) for our model Na_2O surface is that only the Na_2O (110) surface among the low Miller index Na_2O surfaces contains both Na and O atoms, which seems the simplest and most favorable scenario for H_2 molecular adsorptions on the Na_2O surface when forming the product. We begin with the first-principles calculations that determine the energetically preferred structures of the H_2 molecule adsorbed on the Na_2O (110) surface, which reveals the existence of the Na−$H^{\delta-}$···$H^{\delta'+}$−O dihydrogen bond. The molecular dynamics simulation is then employed to provide a view of the dissociation of the H···H bond at elevated temperature.

2. Theoretical Methods

The first-principles calculation has been performed using the Vienna ab initio simulation program, VASP.[12−15] A nine-layer slab, separated by a vacuum layer of 14 Å, is used to model the Na_2O surface (with the calculated lattice constants mentioned below). H_2 molecules are symmetrically put on both sides of the slab to avoid any artificial dipole−dipole interaction between the periodic images in the direction normal to the surface. The Monkhorst−Pack scheme[16] with $4 \times 4 \times 1$ k points ($7 \times 7 \times 7$ for bulk calculation) has been used for integration in the surface Brillouin zone for the $p(2 \times 2)$ supercell. The energy cutoff for the plane waves is 450 eV. The Fermi level is smeared by the Gaussian method[17] with a width of 0.2 eV. We used ultrasoft Vanderbilt-type pseudopotentials[18] as supplied by Kresse and Hafner.[19] The generalized gradient approximation by Perdew and Wang (PW91)[20] is used for the exchange-correlation energy. This set of parameters assures a total energy convergence of 2 meV per atom. During the structural search, all of the atoms are simultaneously relaxed. The search is stopped when forces on all atoms are less than 0.02 eV/Å. An ab initio molecular dynamics (MD) simulation based on the NVT ensemble has also been performed to understand the effect of the temperature on the dihydrogen bond. The time step used for the simulations was 2×10^{-15} s, and the results from the 1.5 ps simulations are reported here.

The potential energy surface of the two-molecule reaction, $Na_2O + H_2 \rightarrow NaH + NaOH$, was analyzed at the B3LYP/6-311+G(d) level using the Gaussian 03 program.[21] The geometries were fully optimized, and the vibrational frequencies were

* Corresponding author. E-mail: q.xu@aist.go.jp.
† AIST.
‡ Toyota Motor Corp.

10.1021/jp065931x CCC: $37.00
Published on Web 03/10/2007

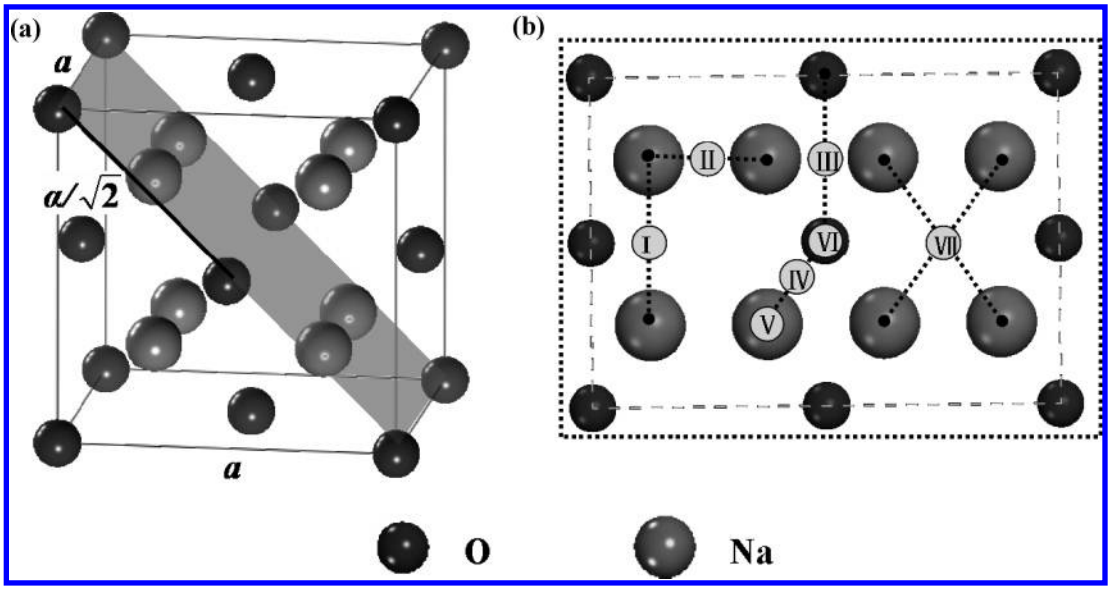

Figure 1. Schematic view of (a) the Na_2O bulk (the (110) cleave plane is highlighted, and the bulk lattice constant is represented by *a*) and (b) the adsorption sites for H_2 on the $p(2 \times 2)$ Na_2O (110) surface.

calculated using analytical second derivatives. The transition-state optimizations were done using the QST3 algorithm within the synchronous transit-guided quasi-Newton (STQN) method, followed by the vibrational calculations showing the obtained structures to be true saddle points. The intrinsic reaction coordinate (IRC) method was used to track the minimum energy paths from the transition structures to the corresponding local minima. A step size of 0.1 amu$^{1/2}$ bohr was used in the IRC procedure.

3. Results and Discussion

Our calculated bulk lattice constant for Na_2O is 5.5278 Å (a_0) in GGA, in good agreement with the experimental value of 5.55 Å.[22] The optimized Na_2O unit cell for the bulk is used to construct the surface supercell. Schematic views of the Na_2O bulk and the (110) cleave plane are shown in Figure 1a. It can be readily seen that both the Na atoms and the O atom are exposed (the ratio of Na to O is 2:1), which is preferable for a further study of the structural rearrangement and reactivity. The Na_2O $p(2 \times 2)$ (110) surface supercell is employed in the present study. To fully investigate absorption and reactivity of H_2 on the surface, all seven possible sites on the surface for H_2 are initially considered to attain an energetically stable structure, including the four bridge sites (I, II, III, and IV), two top sites (V and VI), and one hollow site (VII), as shown in Figure 1b. Calculations allow all layers in the slab to relax, and the results reveal that changes in the topmost interlayer spacing and the core interlayer spacing are all much lower than 3% and 1%, respectively, which is enough to ensure us the accuracy of the result we discussed. That is to say, the above-mentioned slab thickness and the number of atomic layers are sufficient for achieving the total energy and other ground-state properties.

After full optimization, we finally obtained the adsorption configurations of H_2 on the Na_2O (110) surface. Their schematic adsorption structures are shown in Figure 2, and all of the distances between the concerned atoms are listed in Table 1. The energies of the studied seven structures (I−VII) are −420.61316, −418.88525, −418.92228, −420.76899, −418.95686, −419.24135, and −418.91433 eV, respectively. On the basis of their energies, the seven structures can be divided into two groups. Both of the adsorption structures (I and IV) in the lower energy group have the characteristic that one H atom

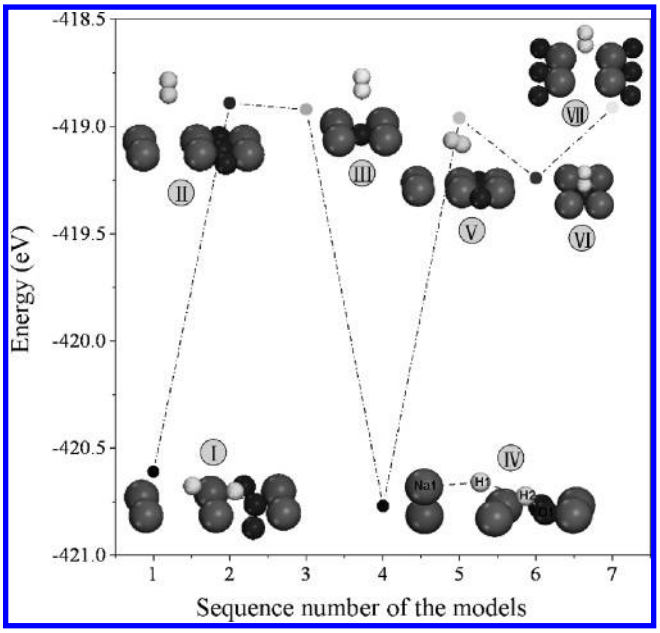

Figure 2. Schematic representation of the seven resultant adsorption structures of hydrogen on the Na_2O (110) surface and their energies.

(represented by H1) bonds to a Na atom (Na1, hereafter denoting the nearest Na atom close to the H1 atom) and the other H atom (represented by H2) bonds to O (O1, hereafter denoting the nearest O atom close to the H2 atom). On the contrary, on the basis of the distances between the concerned atoms as listed in Table 1, in the other five, there is only one hydrogen atom bonded to the surface metal atom (VI) or both hydrogen atoms escape from the surface (II, III, V, and VII). For clarity, hereafter, we only discuss the most energetically stable one, model IV, derived from H_2 at the bridge site of the Na atom and O atom. With a view to the difference in the coordinating environment between the surface and crystal, the distances of Na1−H1 (2.131 Å) and H2−O1 (0.984 Å) that we obtained here were found to be comparable to those in NaH (2.445 Å) and NaOH (0.931 Å), respectively. More interestingly, the distance between the two H (H1 and H2) atoms is 1.766 Å, which is much shorter than the normal H···H contact of 2.4 Å[7] and much longer than the bond length in the free H_2 (0.74611

TABLE 1: Comparison of the Distances/Bond Lengths (in Units of Å) between Na1 and H1, H1 and H2, and H2 and O1 from the Results of First-Principles Calculation of Hydrogen Adsorbed on the Na_2O (110) Surface[a]

	model sequence	Na1−H1	H1−H2	H2−O1
	model 1	2.419	1.724	0.988
	model 2	2.951	0.762	4.846
	model 3	5.472	0.763	3.494
one-H_2	model 4	2.131	1.766	0.984
	model 5	3.072	0.764	3.684
	model 6	3.104	1.284	1.042
	model 7	2.945	0.764	5.401
NaH[b]		2.445		
NaOH[c]		2.710		0.931
four-H_2[d]		2.405	1.891	0.980
four-H_2[e]		2.418	1.905	0.979
molecular dynamics[f]		2.232	2.364	0.978
single molecule[g]		1.889	0.742	0.957

[a] The Na1 and O1, as shown in Figure 2, represent the nearest Na atom and O atom bonded to each H atom, respectively. [b] Experimental data. See ref 27. [c] Experimental data. See ref 28. [d] The first dihydrogen bond when four-H_2 is adsorbed on the surface. [e] The second dihydrogen bond when four-H_2 is adsorbed on the surface. [f] The average bond length of the entire 1.5 ps results. [g] Bond lengths in single molecule NaH, H_2, and NaOH from Gaussian calculation.

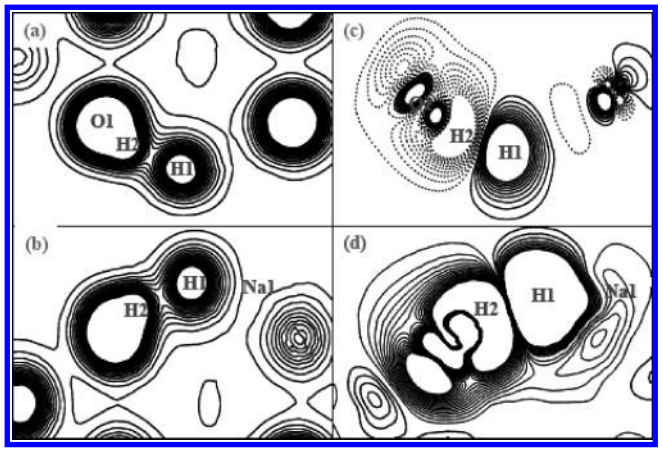

Figure 3. Total (left) and difference (right) charge distributions (a and c) on a plane through the H1, H2, and O1 atoms and (b and d) on a plane through the H1, H2, and Na1 atoms. Contours of the total charge density (a and b) are plotted from 0 to 0.5 e/Å^3 with a spacing of 0.025 e/Å^3. Contours of the different charge density are plotted (c) from −0.02 to 0.01 e/Å^3 with a spacing of 0.0012 e/Å^3 and (d) from −0.05 to 0.05 e/Å^3 with a spacing of 0.005 e/Å^3. In (c) and (d), the positive contours (solid lines) denote the charge accumulation, and negative contours (dotted lines) indicate the charge depletion.

Å).[23] Previous theoretical calculations of systems such as BH_4^-···HCN, LiH···NH_4^+, LiH···HCN, BeH_2···NH_4^+, and BeH_2···HCN have revealed that a dihydrogen bond may have the short bond length of 1.709 Å,[24,25] whereas, to the best of our knowledge, there have been no such reports on material surfaces. Is this attractive Na−H···H−O interaction that we obtained a dihydrogen bond? To validate it, we further analyzed their electronic structures. Figure 3a and b shows the charge density on the planes through H1, H2, and O1, and H1, H2, and Na1, respectively. It was found that there is a remarkable charge overlap between the O (O1) and H (H2) atoms, and the H (H1) and H (H2) atoms, indicating the existence of the O−H and H−H orbital hybridizations, whereas the charge overlap between Na (Na1) and its nearest neighboring H (H1) atoms is rather weak. To obtain thorough insight into the chemical bonding, we examined the charge redistribution, obtained by subtracting the superposed charge density of two H atoms and substrate with the same spatial coordinates as in the slab from the total charge density of the slab. Figure 3c and d shows the spatial redistribution on the planes through the H1, H2, and O1 atoms and H1, H2, and Na1 atoms, respectively. It can be clearly seen that there exists a charge depletion around the Na1 and H2 atoms and the charge accumulation around the O1 and H1 atoms. In other words, charge transfers occur from H2 to its nearest neighboring O1 and from Na1 to its nearest neighboring H1, indicating the strong ionic character of the chemical bonding. This means that the H2 atom bonding to the O1 atom is positively charged ($H^{\delta'+}$) and the H1 atom bonding to the Na1 atom is negatively charged ($H^{\delta-}$), which is necessary for the formation of the dihydrogen bond.

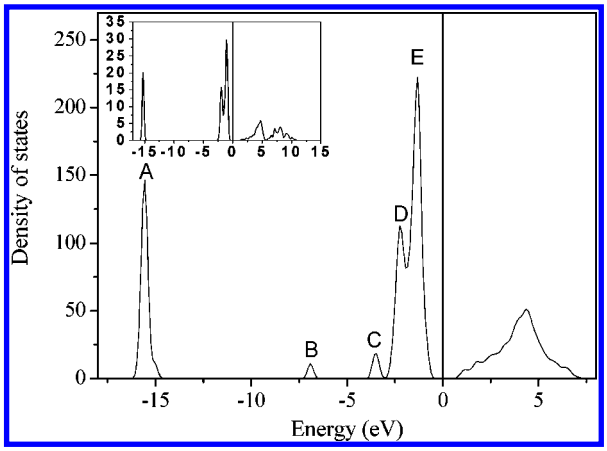

Figure 4. Electronic density of states of the hydrogen absorbed surface and bulk Na_2O (inset at top left corner). The Fermi level is set at zero energy and marked by the vertical lines.

To give further insight into the interaction when hydrogen is adsorbed on the Na_2O (110) surface, the electronic density of states (DOS) of the hydrogen adsorbed surface and bulk Na_2O are provided in Figure 4. Interestingly, two new peaks (B and C), in the energy range from −7.5 to −3 eV, appear for the hydrogen absorbed surface, as compared to the case of the bulk Na_2O, which is more direct evidence for the interaction between hydrogen and a surface. Using the eigen vectors in each energy region of each peak, we can analyze the nature of the electronic states corresponding to each peak. The partial charge density corresponding to each peak in the DOS plot is shown in Figure 5, giving us insight into the bonding of the concerned atoms, Na1, H1, H2, and O1. Peak A mainly comes from the O-2s states. It was found that the strong and weak interactions between the H (H1) and O (O1) atoms result in the occurrence of peaks B and C, and these two peaks also contain the hybridization with the two nearest neighboring H (H1 and H2) atoms. The weak hybridization between H (H1) and Na (Na1) is represented by peak D, and peak E seems to have no bonding character with negligible bonding charges between the H (H2), O (O1), and H (H1) atoms. This information we obtained gives us enough evidence to confirm the Na−$H^{\delta-}$···$H^{\delta'+}$−O dihydrogen bond for the hydrogen storage of Na_2O that we found for the first time. It should be noted that the dihydrogen bond in our case is close to the Crabtree-type dihydrogen bond,[5−7] not the Kubas-type dihydrogen bond,[26] because the two H···H atoms here carry partially positive and negative charges, respectively. The above results are obtained for the situation of one-hydrogen molecule absorption on Na_2O (110) surface. How about multi-hydrogen molecule adsorption on the surface? It was found that only four hydrogen molecules can be located on the surface at the same time, and their initial positions are a geometric similitude relative to the Na and O atoms as it is in the most energetically stable model (IV). As expected, after full

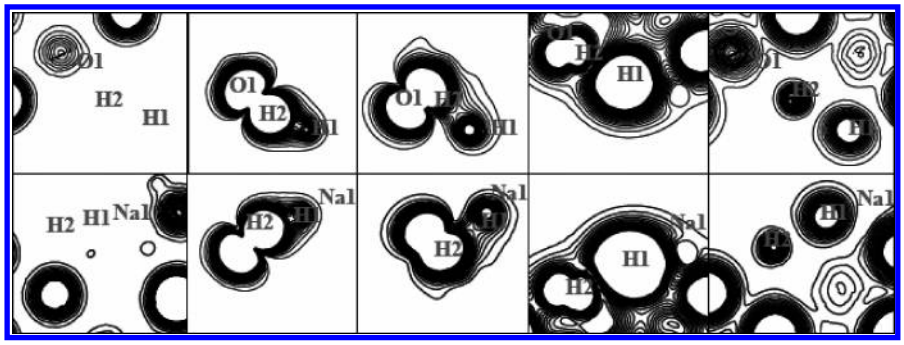

Figure 5. Spatial distributions of the electronic states corresponding to each peak of the DOS plot (from left to right corresponding to peaks A−E in Figure 4) for hydrogen adsorbed on the Na_2O (110) surface in a plane with Na and two H atoms (H1−H2−O1), O and two H atoms (H2−H1−Na1), respectively. Top: H−H−O. Bottom: H−H−Na. Contours of the charge density are plotted from 0 to 0.05 e/Å^3 with a spacing of 0.0025 e/Å^3.

relaxation, two similar dihydrogen bonds are formed, and their bond parameters are also listed in Table 1, which are comparable to those of the one-hydrogen molecule absorbed on the surface. It is noted that the other two hydrogen molecules do not form dihydrogen bonds at the same time, which may be due to a too strong interaction if they all exist in the form of the dihydrogen bond.

The above findings, which confirm the existence of the Na−H$^{\delta-}$···H$^{\delta'+}$−O dihydrogen bond, are obtained at 0 K. Can this dihydrogen bond dissociate, which is very important for the formation of the products, NaH and NaOH, at elevated temperature? To address this question, we carried out a first-principle molecular dynamics calculation at the same temperature as we experimentally used for the hydrogenation of Na_2O, starting from the minimum-energy chemisorption structure. Because of the limited computer time, only the results of a 1.5 ps simulation are provided here. The bond length distributions in the adsorption structure of the one-hydrogen molecules on Na_2O (110) surface were calculated for the different atom pairs, H1−H2, Na1−H1, and H2−O1, as shown in Figure SI-1 and Table 1. It can be easily seen that the bond length between H1−H2 sharply increases at 400 K in comparison to that at 0 K; for example, the average bond length at 400 K is 2.364 Å, which is 0.598 Å longer than that at 0 K (1.766 Å). This gives us definitive evidence of the dissociation of the dihydrogen bond. Furthermore, the average Na1−H1 bond length is 2.232 Å; this value is in the range of its bond length in crystallized NaH, 2.445 Å,[27] and molecular NaH, 1.889 Å (see Gaussian results in the Supporting Information). This is reasonable because the special coordination environment of surface presumably falls into the scope of bulk crystal and single molecule states. The distance of H2 and O1 decreases toward that in the bulk NaOH[28] and molecular one. On the basis of the variation in the bonds, we can reasonably suppose that there is a strong tendency for decomposition of the hydrogen on the surface and the formation of Na1−H1 and O1−H2 bonds, which occurs during the formation of sodium hydride and sodium hydroxide.

To gain insight into the role of the dihydrogen bond in the reaction of the Na−O−H system, we have also performed two-molecule-model reaction processes using the Gaussian package. The optimized structures of the reaction products, intermediates, and transition states are shown in Figure 6. Figure 7 schematically presents the potential energy surface for the $Na_2O + H_2 \rightarrow NaH + NaOH$ reaction.

As shown in Figure 7, during the first reaction step, the H_2 molecule approaches the Na_2O molecule to form the Na_2O (η^2-H_2) complex without an energy barrier. It is predicted that the Na_2O (η^2-H_2) complex lies 27.49 kcal/mol lower in energy than the reactants. From Na_2O (η^2-H_2), the reaction proceeds by

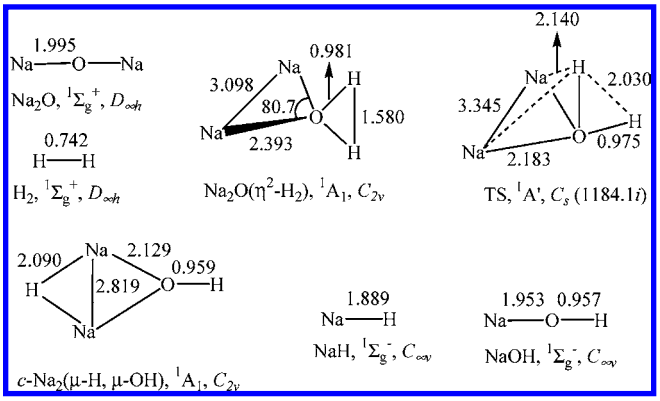

Figure 6. Optimized structures (bond lengths in angstroms, bond angles in deg), electronic ground state, and point group for the reactants, intermediates, transition state, and products of the $Na_2O + H_2 \rightarrow NaH + NaOH$ reaction. For the transition state (TS), the letter "i" denotes the imaginary frequency (in cm^{-1}).

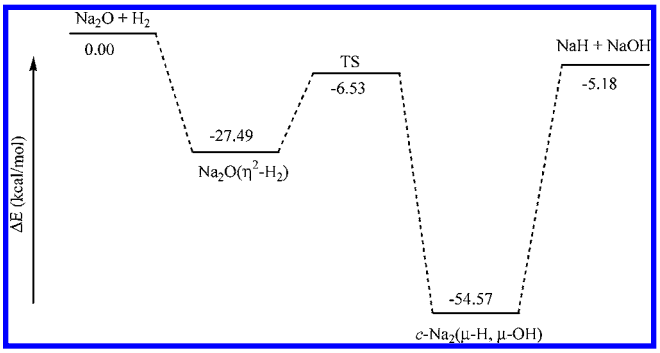

Figure 7. Potential energy surface for the $Na_2O + H_2 \rightarrow NaH + NaOH$ reaction calculated at the B3LYP/6-311+G(d) level.

migration of one of the hydrogen atoms to form a planar *c*-Na_2(μ-H, μ-OH) via the transition state, TS. The H−H distance in the TS is 2.030 Å (Figure 6), which is 0.450 Å longer than that in Na_2O (η^2-H_2). The barrier for this process is predicted to be 20.96 kcal/mol (Figure 7). The vibrational mode of the imaginary frequency of TS (1184.1i cm^{-1}) corresponds to the transition motion leading to the H−H cleavage. The transition-state optimization was followed by the frequency and IRC calculations, which confirmed that TS does connect Na_2O(η^2-H_2) and *c*-Na_2(μ-H, μ-OH). The *c*-Na_2(μ-H, μ-OH) molecule lies 54.57 kcal/mol lower in energy than the NaH and NaOH products. Meanwhile, the $Na_2O + H_2 \rightarrow NaH + NaOH$ reaction is predicted to be slightly exothermic (5.18 kcal/mol). The B3LYP calculations provided evidence for the existence of the double hydrogen bond during the dissociation of the H_2 molecule, which is consistent with the VASP calculations.

4. Conclusions

For the first time, an ab initio molecular dynamics simulation confirmed the existence and dissociation of the dihydrogen bond on a metal oxide surface. These results will assist with the ongoing experiments to understand the reaction mechanism and improve the performance of the safe, contamination-free, and easy-to-handle Na−O−H system to meet practical applications. Our results would open a door for understanding related hydrogenation/dehydrogenation systems such as Li−N−H and lead to the finding of new hydrogen storage materials.

Acknowledgment. We sincerely thank the reviewers for valuable suggestions. This work was financially supported by AIST and Toyota Motor Co. X.-B.Z. thanks JSPS for a fellowship.

Supporting Information Available: Bond length distributions in the adsorption structure of one-hydrogen molecule adsorbed on the Na_2O (110) surface from the MD simulation. This material is available free of charge via the Internet at http://pubs.acs.org.

References and Notes

(1) Schlapbach, L.; Zuttel, A. *Nature* **2001**, *414*, 353.

(2) Chen, P.; Xiong, Z. T.; Luo, J. Z.; Lin, J. Y.; Tan, K. L. *Nature* **2002**, *420*, 302.

(3) Stevens, R. C.; Bau, R.; Milstein, D.; Blum, O.; Koetzle, T. F. *J. Chem. Soc., Dalton Trans.* **1990**, 1429.

(4) Van der Sluys, L. S.; Eckert, J.; Eisenstein, O.; Hall, J. H.; Huffman, J. C.; Jackson, S. A.; Koetzle, T. F.; Kubas, G. J.; Vergamini, P. J.; Caulton, K. G. *J. Am. Chem. Soc.* **1990**, *112*, 4831.

(5) Richardson, T. B.; de Gala, S.; Crabtree, R. H.; Siegbahn, P. E. M. *J. Am. Chem. Soc.* **1995**, *117*, 12875.

(6) Crabtree, R. H.; Siegbahn, P. E. M.; Eisenstein, O.; Rheingold, A. L.; Koetzle, T. F. *Acc. Chem. Res.* **1996**, *29*, 348.

(7) Crabtree, R. H. *Science* **1998**, *282*, 2000.

(8) Xu, Q.; Wang, R. T.; Kiyobayashi, T.; Kuriyama, N.; Kobayashi, T. *J. Power Sources* **2006**, *155*, 167.

(9) Peles, A.; Alford, J. A.; Ma, Z.; Yang, L.; Chou, M. Y. *Phys. Rev. B* **2004**, *70*, 165105.

(10) Aguayo, A.; Singh, D. J. *Phys. Rev. B* **2004**, *69*, 155103.

(11) Chaudhuri, S.; Muckerman, J. T. *J. Phys. Chem. B* **2005**, *109*, 6952−6957.

(12) Kresse, G.; Hafner, J. *Phys. Rev. B* **1993**, *47*, RC558.

(13) Kresse, G.; Furthmuller, J. *Phys. Rev. B* **1996**, *54*, 11169.

(14) Kresse, G.; Hafner, J. *Phys. Rev. B* **1994**, *49*, 14251.

(15) Pasquarello, A.; Laasonen, K.; Car, R.; Lee, C. Y.; Vanderbilt, D. *Phys. Rev. Lett.* **1992**, *69*, 1982.

(16) Monkhorst, H. J.; Pack, J. D. *Phys. Rev. B* **1976**, *13*, 5188.

(17) Methfessel, M.; Paxton, A. T. *Phys. Rev. B* **1989**, *40*, 3616.

(18) Vanderbilt, D. *Phys. Rev. B* **1990**, *41*, 7892.

(19) Kresse, G.; Hafner, J. *J. Phys.: Condens. Matter* **1994**, *6*, 8245.

(20) Perdew, J. P.; Wang, Y. *Phys. Rev. B* **1992**, *45*, 13244.

(21) Frisch, M. J.; Trucks, G. W.; Schlegel, H. B.; Scuseria, G. E.; Robb, M. A.; Cheeseman, J. R.; Montgomery, J. A., Jr.; Vreven, T.; Kudin, K. N.; Burant, J. C.; Millam, J. M.; Iyengar, S. S.; Tomasi, J.; Barone, V.; Mennucci, B.; Cossi, M.; Scalmani, G.; Rega, N.; Petersson, G. A.; Nakatsuji, H.; Hada, M.; Ehara, M.; Toyota, K.; Fukuda, R.; Hasegawa, J.; Ishida, M.; Nakajima, T.; Honda, Y.; Kitao, O.; Nakai, H.; Klene, M.; Li, X.; Knox, J. E.; Hratchian, H. P.; Cross, J. B.; Adamo, C.; Jaramillo, J.; Gomperts, R.; Stratmann, R. E.; Yazyev, O.; Austin, A. J.; Cammi, R.; Pomelli, C.; Ochterski, J. W.; Ayala, P. Y.; Morokuma, K.; Voth, G. A.; Salvador, P.; Dannenberg, J. J.; Zakrzewski, V. G.; Dapprich, S.; Daniels, A. D.; Strain, M. C.; Farkas, O.; Malick, D. K.; Rabuck, A. D.; Raghavachari, K.; Foresman, J. B.; Ortiz, J. V.; Cui, Q.; Baboul, A. G.; Clifford, S.; Cioslowski, J.; Stefanov, B. B.; Liu, G.; Liashenko, A.; Piskorz, P.; Komaromi, I.; Martin, R. L.; Fox, D. J.; Keith, T.; Al-Laham, M. A.; Peng, C. Y.; Nanayakkara, A.; Challacombe, M.; Gill, P. M. W.; Johnson, B.; Chen, W.; Wong, M. W.; Gonzalez, C.; Pople, J. A. *Gaussian 03*, revision B.04; Gaussian, Inc.: Pittsburgh, PA, 2003.

(22) Zintl, E.; Harder, A.; Dauth, B. *Z. Elektrochem.* **1934**, *40*, 588.

(23) Weast, R. C.; Astle, M. J.; Beyer, W. H. *CRC Handbook of Chemistry and Physics*; CRC Press: Boca Raton, FL, 1986−1987; pp F159.

(24) Bennett, S. L.; Field, F. H. *J. Am. Chem. Soc.* **1972**, *94*, 5188.

(25) Bennett, S. L.; Field, F. H. *J. Am. Chem. Soc.* **1972**, *94*, 6305.

(26) Kubas, G. J.; Ryan, R. R.; Swanson, B. I.; Vergamini, P. J.; Wasserman, H. J. *J. Am. Chem. Soc.* **1984**, *106*, 451.

(27) Shull, C. G.; Wollan, E. O.; Morton, G. A.; Davidson, W. L. *Phys. Rev.* **1948**, *73*, 842.

(28) Beck, H. P.; Lederer, G. *Phase Transitions* **1992**, *38*, 127.